HYDROGEN, FUEL CELL & ENERGY STORAGE

Optimal Design of a Fractional-Order Controller for Stabilization and Control of DC Microgrids in the Presence of Constant Power and Voltage Loads Using a Grey Wolf Optimization Algorithm

Narges Jahantiqh | **Mojtaba Shivaie***

Department of Electrical Engineering, Shahrood University of Technology, Shahrood, Iran
* Corresponding author, Email: shivaie@shahroodut.ac.ir

Article Information

Article Type
Research Article

Article History
Received: *10 Dec 2024*
Revised: *12 Feb 2025*
Accepted: *02 Mar 2025*
Published Online: *04 Mar 2025*

Keywords

Constant power load
Constant voltage load
DC microgrid
Fractional order controller
Gray wolf algorithm
Noise and disturbances

Abstract

This paper presents a new optimal design of a fractional order controller for the control and stabilization of DC microgrids, particularly under constant power and voltage loads. The study focuses on a well-designed DC microgrid configuration, including two buck-boost power electronic converters, a constant power load, and a constant voltage load. The proposed microgrid operates with a total power consumption of 2 kW, an input voltage of 100 V for the converters, and a DC bus voltage of 250 V. The fractional order controller parameters are optimized using a robust gray wolf optimization algorithm, chosen for its superior performance in handling complex optimization problems compared to other methods. The functionality of the controller is evaluated under various noise and disturbance conditions to ensure the stability of the DC bus. Additionally, the proposed fractional order controller is benchmarked against a conventional proportional-integral-derivative (PID) controller under different operating conditions. The simulation results highlight the enhanced stability and control offered by the fractional order controller, demonstrating its practical applicability in real-world DC microgrids.

Cite this article: Jahantigh, N., Shivaie, M., (2025). Optimal Design of a Fractional-Order Controller for Stabilization and Control of DC Microgrids in the Presence of Constant Power and Voltage Loads Using a Grey Wolf Optimization Algorithm. DOI: 10.22104/hfe.2024.7105.1317

 Publisher: Iranian Research Organization for Science and Technology (IROST)
DOI: 10.22104/hfe.2024.7105.1317

1 Introduction

1.1 Background and motivation

The utilization of DC microgrids has become increasingly significant due to the proliferation of distributed energy resources located in close proximity to electrical energy consumers. Currently, DC microgrids are employed in various applications, including commercial and residential buildings as well as industrial units [1, 2]. In DC microgrids, constant power load connections to the DC bus are common. The control of constant power loads is achieved through power electronic converters, which are designed with a sufficiently wide bandwidth to ensure that the power consumption remains relatively independent of voltage variations [3]. Constant power loads exhibit a negative impedance characteristic when connected to the DC bus, leading to voltage drops across the converters and reduced bus stability. Therefore, ensuring the stability of the DC bus connected to a constant power load and maintaining a desired output voltage is paramount. To clarify the distinction between existing control strategies and the proposed FOPID controller, it is essential to highlight the main gaps in conventional methods. Traditional PID controllers often struggle with handling non-linearity and time-varying dynamics in microgrid systems. They may also lack the flexibility to adapt to varying operational conditions. In contrast, the FOPID controller offers enhanced robustness and adaptability by incorporating fractional calculus, which allows for more precise tuning and better performance in complex environments. This sets the stage for introducing the proposed FOPID solution as a superior alternative. Employing fractional-order controllers to address the uncertainties associated with constant power loads can enhance DC bus stability. Recently, the application of fractional-order controllers in controlling power electronic converters has gained significant traction [4, 5]. Advantages of fractional-order controllers over conventional controllers include (1) greater flexibility, (2) simpler design for higher-order converters, (3) enhanced robustness and stability, and (4) the elimination of the need for linearization [6, 7].

1.2 Literature review

The advantages of utilizing DC microgrids include reduced costs, the elimination of transmission lines due to the short distance between generators and consumers, improved power quality resulting from the integration of power electronic converters on the load side, simplified energy generation systems, and the ability to create multiple voltage levels without the need for transformers [8, 9]. However, due to the presence of uncertainties in the system, input voltage fluctuations, disturbances, and parameter variations in microgrids, conventional controllers exhibit inadequate performance and fail to ensure system stability [10]. In islanded microgrids, power electronic converters play a crucial role in supplying local loads. Consequently, various control strategies, such as droop control and master-slave control, have been proposed to enhance the parallel operation of distributed energy resources and power electronic converters. Nevertheless, these controllers are unable to improve the stability of converters and the DC bus in the presence of constant power loads [11]. Reference [12] employs an active control method along with a nonlinear disturbance observer to ensure stability, regulating the output voltage and maintaining stability against the negative resistance of the constant power load.

Reference [13] utilizes an adaptive active controller for feeding a constant power load using a buck-boost converter, enhancing system stability and adapting the controller to parameter variations to increase DC bus damping. Paper [14] proposes a passive control method, which suffers from drawbacks such as design complexity and practical implementation difficulties. Additionally, reference [15] employs a proportional-integral-derivative (PID) controller with a filter to mitigate the adverse effects of the derivative term and accurately track the output voltage. The controller parameters are calculated using the particle swarm optimization algorithm. In microgrids, the capacitive elements of voltage source converters combined with line inductance form an LC circuit with weak damping, leading to reduced DC bus stability. When feeding constant power loads using DC microgrids, a negative resistance effect is introduced on the DC bus, causing dynamic variations that further decrease bus stability and result in undesirable output voltage fluctuations [16]. Therefore, designing a controller that is robust against constant power load uncertainties, accurately tracks the output using a fractional-order controller in the presence of noise and disturbances, and ensures voltage stability is crucial. Small-signal stability in islanded microgrids is of paramount importance. In this mode, distributed energy resources behave as voltage sources, and the dynamic characteristics of the microgrid are highly dependent on power derating controllers and connected DGs [17].

The primary objectives of microgrid control include maintaining frequency and voltage, distributing power among sources, and enhancing reliability. Under normal operating conditions, the microgrid is connected to the main grid, and its loads are supplied by dis-

tributed energy resources or, if necessary, by the main grid. However, in the event of a disturbance in the main grid, the microgrid can isolate itself from the distribution network to protect microgrid loads from disturbances. Therefore, the ability of a microgrid to island can reduce consumer outage time and ultimately increase system reliability [3, 18, 19].

1.3 Aims and contributions

In this paper, a novel fractional-order controller is designed to control and stabilize a DC microgrid in the presence of constant power and voltage loads, considering noise and disturbances. The proposed approach enables the fractional-order controller to exhibit effective performance under various input fluctuations of solar panels, noise, and disturbances. Considering the power exchange between microgrids and the upstream grid, microgrid operation can be classified as either standalone or grid-connected. In the standalone mode, there is no connection between the microgrid and the main grid, and the microgrid must be self-sufficient, making distributed energy resources crucial. In contrast, grid-connected microgrids have the support of the upstream grid [18–20]. Accordingly, microgrid control can be categorized into centralized and decentralized approaches [8, 21].

From the perspective of the upstream grid, a microgrid resembles a combined energy generation unit or a load. In other words, a microgrid is a power distribution system that automatically provides power with appropriate quality and reliability to supply loads [18]. Based on the literature review and problem statement, the novelties of this paper in the field of DC bus control and stability in the presence of noise and disturbances are as follows:

- This paper presents a standalone DC solar panel microgrid with variable solar irradiance and temperature inputs and an output voltage of approximately 100 volts.
- A buck-boost power electronic converter connected to the DC solar panel is modeled and employed to interface with the bus while providing appropriate output values under varying conditions.
- The load is modeled as a constant power and constant voltage load connected to the DC bus and the buck-boost converter to represent power consumption and voltage levels.
- Both fractional-order and proportional-integral-derivative (PID) controllers are employed to maintain stability against noise.
- A grey wolf optimization algorithm is utilized to optimize the controller parameters for superior performance compared to the conventional PID controller.

This paper is organized into six sections. Section 2 presents the modeling of buck and boost converters, as well as constant power and constant voltage loads. In section 3, the controller design is investigated. Section 4 outlines the problem-solving approach for controller optimization. Section 5 presents a case study and simulation results, followed by a discussion. Finally, section 6 concludes the paper.

2 Buck-Boost Converter Modeling

Power electronic converters are crucial components of microgrids, playing a vital role in controlling power distribution and converting power to suitable AC or DC forms. They also serve as interfaces, connecting variable speed generators, energy storage systems, and DC distributed energy resources to the grid [22]. In islanded microgrids, power electronic converters play a pivotal role in ensuring the continuous supply to local and critical loads. Consequently, various control methods such as droop control and master-slave control have been proposed to enable the parallel operation of distributed energy resources based on power electronic converters [23].

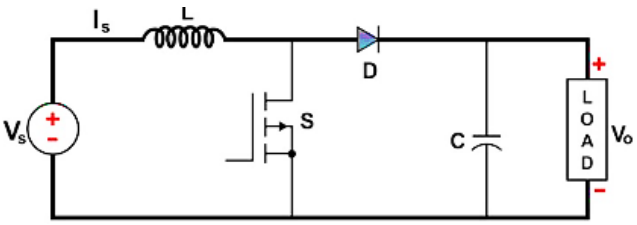

Fig. 1. Boost converter.

2.1 DC-DC Boost converter

This converter is a boost converter, always regulating the output voltage higher than the input voltage. It is used to regulate the output voltage of DC sources and control the DC bus voltage. Figure 1 shows a schematic of a boost converter. A boost converter is a switching-based converter. By increasing the duty cycle, high gains can be achieved, as evident from Equation (1).

$$\frac{V_O}{V_S} = \frac{1}{1-D}\,. \tag{1}$$

In this equation, V_O and V_S represent the output and input voltages of the converter, respectively, and D represents the duty cycle. By increasing the duty cycle,

very high gains can be obtained. In practice, the maximum gain achievable from a typical boost converter is around 5 to 6 times [12, 24].

2.2 Buck DC-DC converter

In this converter, the output voltage is always regulated to a value lower than the input voltage. Furthermore, since the operation of these converters is based on switching, the output voltage of these converters always contains harmonics. To mitigate this issue, a low-pass filter consisting of an inductor and a capacitor is used. A complete schematic of a Buck converter is shown in Figure 2.

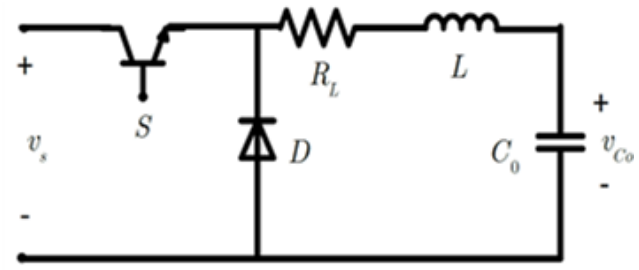

Fig. 2. Buck Converter.

Buck converters with pulse width modulation (PWM) are widely used in battery chargers, radio systems, computers, telecommunications equipment, fuel cells, and more [24]. In this paper, a buck converter is used to simulate a constant power load in small signal stability analysis. Equation (2) represents the ratio of output voltage to input voltage in a buck converter.

$$\frac{V_O}{V_S} = D \tag{2}$$

where V_O and V_S represent the output voltage and input voltage of the converter, respectively, and D represents the duty cycle of the converter.

2.3 Load modeling in DC microgrids

In general, loads in DC microgrids can be categorized into three main types: constant resistance loads (CRL), constant current loads (CCL), and constant power loads (CPL). In this paper, constant resistance loads and constant power loads are investigated based on Equations (3) and (4):

- Constant Resistance Loads

$$i_{\mathrm{CRL}} = \left(\frac{1}{R_{\mathrm{load}}}\right) v = \left(\frac{P_{\mathrm{CRL}}}{V_0^2}\right) v \tag{3}$$

  where R_{load} represents a constant resistive load, V_0 is the nominal voltage, and v, i_{CRL}, and P_{CRL} represent the voltage, current, and power of the constant resistive load, respectively.

- Constant Power Loads

$$i_{\mathrm{CPL}} = \frac{P_{\mathrm{CPL}}}{v} \tag{4}$$

  where v, i_{CPL}, and P_{CPL} represent the voltage, Current, and power of the constant power load, respectively.

3 Fractional-Order Controller Design

The ability of an electrical power system to return to a stable operating condition with bounded variables after being subjected to a physical disturbance from an initial operating condition is known as power system stability [25]. Stability in DC microgrids is examined in three forms: (1) small-signal stability, (2) transient stability, and (3) voltage stability [25].

3.1 State-space modeling and stability analysis

There are various methods for modeling a physical system. One of these methods is the state-space representation, where a set of independent variables, known as state variables, are chosen. At any given time, the state of the system is completely determined by these variables. In the state equations of the system, x represents the state vector of the system, t denotes time, and u represents the input vector of the system. By setting $\dot{X}$ to zero, the operating point of the system is obtained. If the system is linear, the governing equations of the system can be written in the following general form:

$$\dot{\mathsf{X}} = F(x, t, u) \tag{5}$$

$$\mathsf{Y} = G(x, t, u) \tag{6}$$

$$\dot{\mathsf{X}}(t) = \mathsf{A}\mathsf{X}(t) + \mathsf{B}u(t) \tag{7}$$

$$\mathsf{Y}(t) = \mathsf{C}\mathsf{X}(t) + \mathsf{D}u(t) \tag{8}$$

where A is the state matrix, X is the state variable matrix, B and C are the input and output matrices, respectively, and D is the direct transmission matrix between input and output. In a situation where the disturbance applied to the system is small, the values of the state variables will vary around the operating point. To perform a linear analysis of the system, the state equations must be linearized around the operating point. This type of analysis is called small-signal analysis. The state matrix of the system is obtained through the linearized equations. The eigenvalues obtained from this matrix represent the behavior of the

system around the operating point. The small-signal equations of the system can be written as follows:

$$\Delta\dot{\mathsf{X}} = \mathsf{A}\mathsf{X}(t) + \mathsf{B}\mathsf{X}(t) \tag{9}$$

$$\Delta\mathsf{Y} = \mathsf{C}\mathsf{X}(t) + \mathsf{D}\mathsf{X}(t) \tag{10}$$

In this equation, matrices A, B, C, and D represent the coefficient matrices, which are obtained by considering x_0 and u_0 as the system's operating points.

$$\mathsf{A} = \begin{bmatrix} \frac{\partial f_1}{\partial x_1} & \cdots & \frac{\partial f_1}{\partial x_n} \\ \vdots & \cdots & \vdots \\ \frac{\partial f_n}{\partial x_1} & \cdots & \frac{\partial f_n}{\partial x_n} \end{bmatrix}^{x=x_0}_{u=u_0},$$

$$\mathsf{B} = \begin{bmatrix} \frac{\partial f_1}{\partial u_1} & \cdots & \frac{\partial f_1}{\partial u_n} \\ \vdots & \cdots & \vdots \\ \frac{\partial f_n}{\partial u_1} & \cdots & \frac{\partial f_n}{\partial u_n} \end{bmatrix}^{x=x_0}_{u=u_0},$$

$$\mathsf{C} = \begin{bmatrix} \frac{\partial g_1}{\partial x_1} & \cdots & \frac{\partial g_1}{\partial x_n} \\ \vdots & \cdots & \vdots \\ \frac{\partial g_n}{\partial x_1} & \cdots & \frac{\partial g_n}{\partial x_n} \end{bmatrix}^{x=x_0}_{u=u_0},$$

$$\mathsf{D} = \begin{bmatrix} \frac{\partial g_1}{\partial u_1} & \cdots & \frac{\partial g_1}{\partial u_n} \\ \vdots & \cdots & \vdots \\ \frac{\partial g_n}{\partial u_1} & \cdots & \frac{\partial g_n}{\partial u_n} \end{bmatrix}^{x=x_0}_{u=u_0}. \tag{11}$$

The system stability of a DC microgrid is analyzed by examining the eigenvalues of the system matrix A. When all eigenvalues lie in the left half-plane of the complex plane, the system is stable under small perturbations near the equilibrium point. The eigenvalues of matrix A are obtained from the following equation:

$$\det(\mathsf{A} - \lambda\mathsf{I}) = 0 \tag{12}$$

Here, λ represents the eigenvalues of the system, I is the identity matrix, and "det" denotes the determinant.

3.2 Fractional-order controller

When a properly-ordered classical controller is employed, the controller behavior is solely examined based on the three parameters of proportional, integral, and derivative gain, as defined in Equation (13). The proportional-integral-derivative (PID) controller relationship is as follows [26]:

$$U(t) = P + \frac{1}{S} + D \cdot \frac{N}{1 + N \cdot \left(\frac{1}{S}\right)} \tag{13}$$

- **Proportional Term:** This section examines the reduction of steady-state error, maintenance of stability, and increase in response speed.
- **Integral Term:** This section investigates the reduction of stability and the elimination of steady-state error.
- **Derivative Term:** This section explores the increase in sensitivity to noise and the improvement of relative stability.

Various algorithms can be used to tune the parameters of PID controllers [26]. Fractional-order PID controllers are an extension of PID controllers based on fractional calculus. Due to their higher flexibility compared to classical controllers, fractional-order controllers are widely used in many research studies [27]. While classical controllers have three components, fractional-order controllers have five components, resulting in higher accuracy compared to classical controllers [28–30]. The formula for the fractional-order controller is as follows [7,31]:

$$u(s) = P + \frac{I}{S^{\lambda}} + D \cdot S^{\mu} \tag{14}$$

In this equation, λ and μ represent the real powers of the integral and differential operators, respectively [31]. A gray wolf optimization algorithm has been employed to optimize and tune the parameters of the fractional-order controller.

4 Grey Wolf Optimization Algorithm

The Grey Wolf Optimizer (GWO) algorithm is inspired by the hierarchical social structure and hunting behavior of grey wolves [32]. Grey wolves, occupying the apex of the food chain, often live in packs. The alpha wolf holds the highest rank in the pack and is the leader. The beta wolf, ranking second, acts as an advisor to the alpha and follows its commands. Omega wolves hold the lowest rank and often assume the role of caring for the pups. Delta wolves, positioned between the beta and omega wolves, are responsible for guarding, caring for the elderly, and hunting. This hierarchical structure and collaborative hunting behavior have inspired the development of a mathematical model, resulting in the Grey Wolf Optimizer algorithm. The primary stages of grey wolf hunting are as follows [33]: (i) pursuing and approaching the prey; (ii) encircling and harassing the prey until submission; and, (iii) attacking the prey. The gray wolf optimization algorithm offers several advantages when optimizing a fractional order controller. Firstly, GWO is straightforward to implement and adapt to various optimization problems, making it suitable for complex control systems like fractional order controllers. It effectively balances exploration (searching for new solutions) and exploitation

(refining existing solutions), which helps in finding the global optimum more efficiently. Additionally, the algorithm's design mimics the social hierarchy and hunting behavior of gray wolves, aiding in avoiding local optima and ensuring a more thorough search of the solution space. GWO has also demonstrated robust performance under different conditions and disturbances, making it reliable for optimizing controllers in dynamic and uncertain environments. These advantages make GWO a powerful tool for enhancing the performance and robustness of fractional order controllers in various applications. To optimize the proposed controller's values, the algorithm has been calculated in 100 steps and 50 wolves in each neighborhood. The limit of numbers between 0.00001 and 1 has been used for the values of the controller parameters.

5 Case Study and Simulation Results

5.1 PV Array

This simulation uses a DC microgrid powered by solar panels composed of silicon solar cells. The power output depends on solar irradiance and temperature, both of which are variable. Higher irradiance and lower temperatures increase the output power. Figures 3 and 4 illustrate the relationships: Figure 3 shows the linear relationship between irradiance and temperature over time, while Figure 4 demonstrates the increase in voltage and current of the PV Array and diode as irradiance rises. Additionally, the PV Array current increases with rising temperature. Figure 5 presents the irradiation and temperature levels, as well as their corresponding variations.

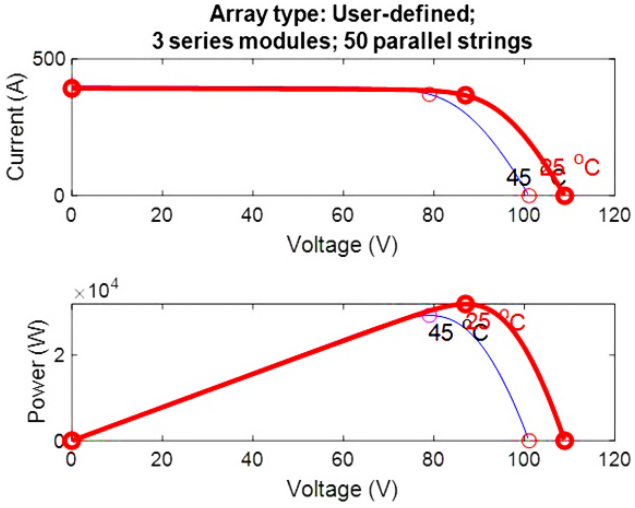

Fig. 3. Characteristics of PV array.

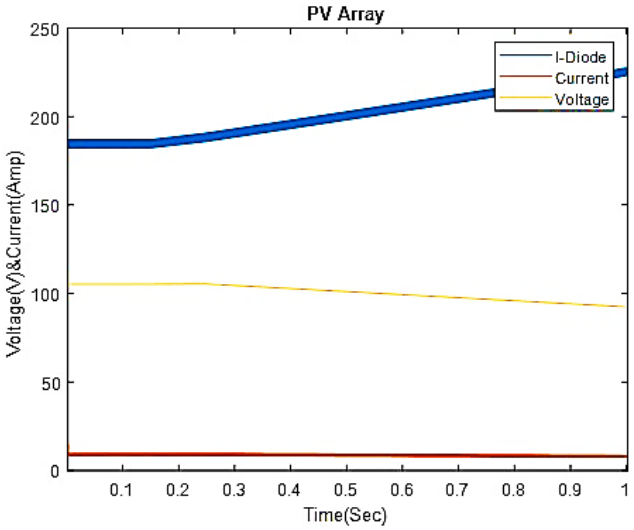

Fig. 4. Current, voltage, and diode current.

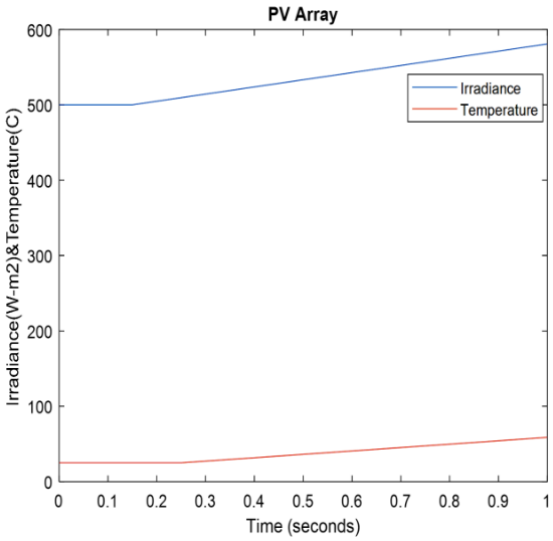

Fig. 5. Irradiance and temperature.

5.2 Buck-boost converter

The buck-boost converter is a DC-DC converter capable of both stepping up and stepping down the output voltage. It consists of a switching transistor, an inductor, a capacitor, and a diode. In PV Array applications, buck-boost converters can be used to boost the output voltage under low-irradiance conditions or to buck the output voltage under high-irradiance conditions. The output voltage of the buck-boost converter is regulated using a controller. The controller compares the output voltage to a reference voltage. If the output voltage is lower than the reference voltage, the controller increases the duty cycle to increase the output voltage. Conversely, if the output voltage exceeds the reference

voltage, the controller decreases the duty cycle to reduce the output voltage. All the simulations have been done in the Simulink environment of MATLAB software with an accuracy of 1 microsecond and in the form of discrete time.

5.3 Scenario 1: Constant Voltage Load

Figure 6 presents a schematic overview of the constant voltage load condition.

A constant voltage load is a load whose power consumption remains constant regardless of changes in input voltage. Essentially, this type of load represents a real-world consumer used in various applications. This paper investigates the performance of a buck-boost converter under a constant voltage load condition. To this end, the line voltage and output voltage of the constant voltage load, along with the power, were measured and analyzed. Figure 7 shows the line voltage curve, which is a horizontal line. This indicates that the line voltage remains constant over time, and even if the input voltage of the buck-boost converter changes, the output line voltage will not change. Considering the output of a PV Array, it is expected that the buck-boost converter can provide a line output voltage of around 250 volts. However, in practice, due to system losses, the output line voltage was around 210 volts. Figure 8 demonstrates the correct operation of the buck-boost converter under a constant voltage load, where the output line voltage is equal to the output of the constant voltage load. Figure 9 shows the output power under a constant voltage load condition.

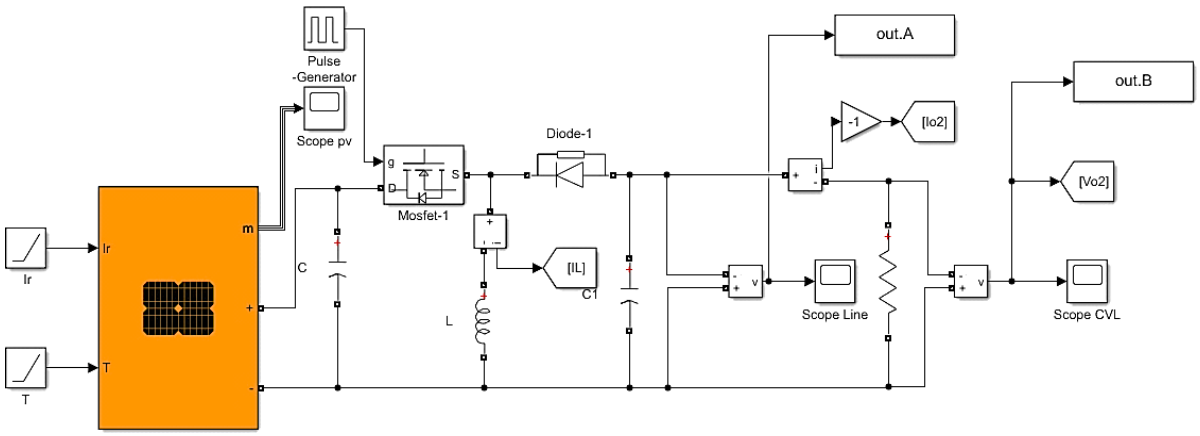

Fig. 6. Constant Voltage Load (CVL).

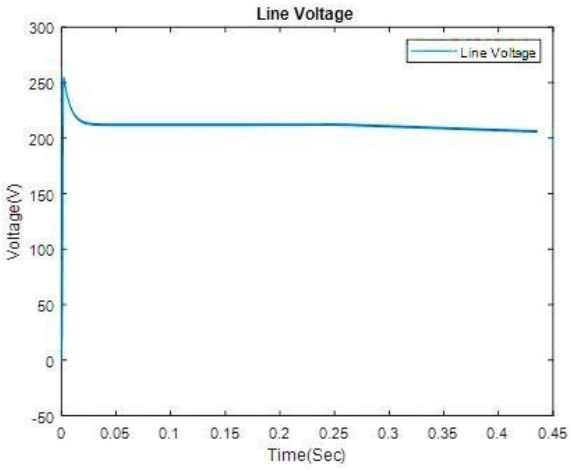

Fig. 7. Voltage line CVL.

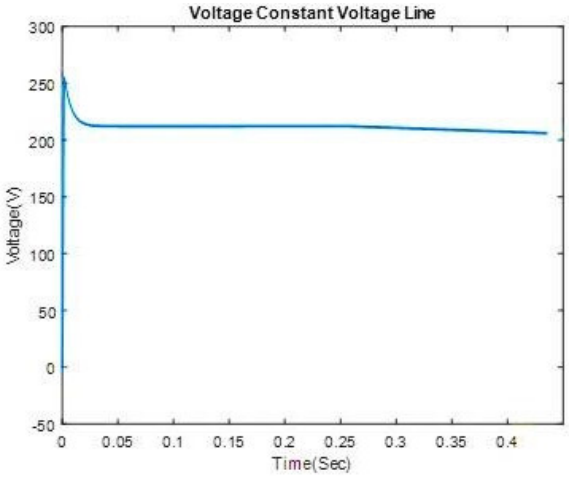

Fig. 8. Output CVL.

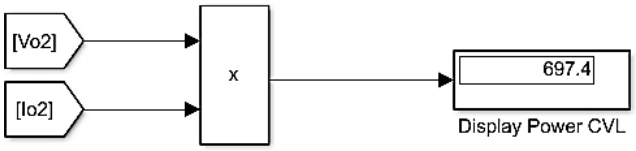

Fig. 9. Power CVL.

5.4 Scenario 2: Constant Power Load

Figure 10 presents a schematic overview of the constant power load condition.

A constant power load is a load whose current is independent of the applied voltage. In other words, the power consumption of this load is proportional to the applied voltage. Constant power loads are used in a wide range of applications. Constant power loads play a significant role in electrical systems.

These loads can have various effects on the system, including increased peak current, reduced voltage, and increased power losses. Figure 11 shows the linear output voltage waveform of a buck-boost converter under constant power load conditions. As can be seen from the figure, the output voltage of the buck-boost converter is constant under constant power load conditions. This is because the output current of the converter is also constant under constant power load conditions. With a constant output current, the output voltage will also be constant. Figure 12 shows the linear output voltage waveform of the constant power load. The input to the constant power load is the same as the output of the line. The constant power load is designed as a buck converter, and since the voltage is constant under constant power load conditions, a constant output is observed after reducing the input by the buck converter. Figure 13 shows the output power under a constant power load condition.

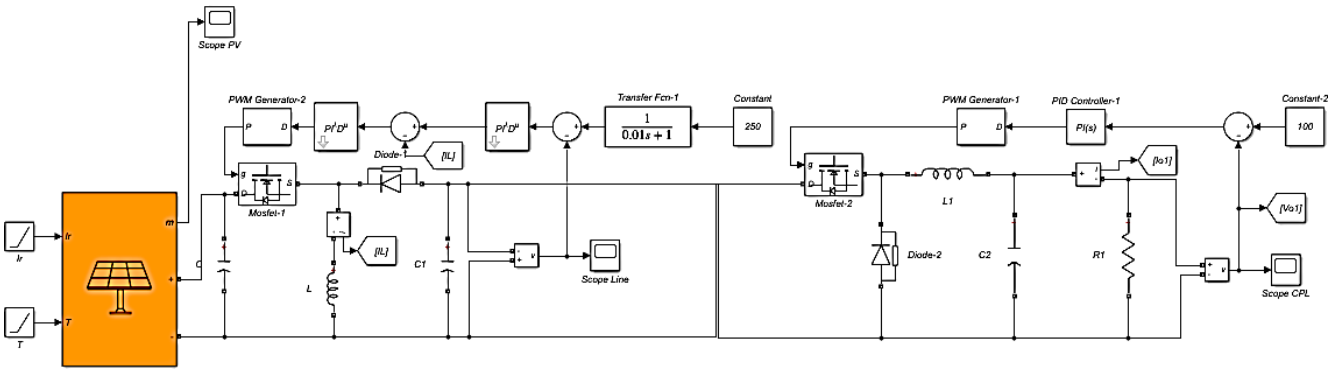

Fig. 10. Constant Power Load (CPL).

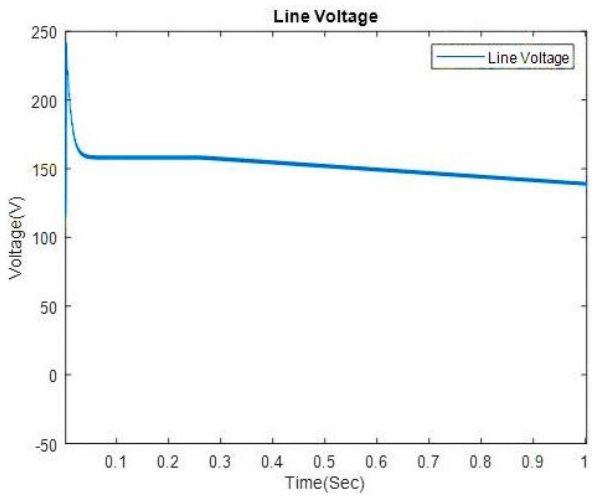

Fig. 11. Voltage Line CPL.

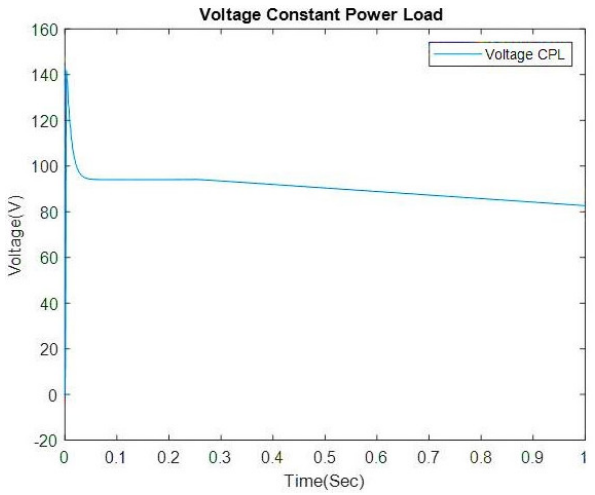

Fig. 12. Output CPL.

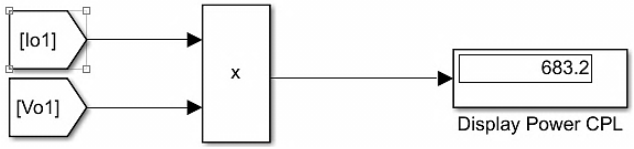

Fig. 13. Power CPL.

5.5 Scenario 3: Constant Power Load with Constant Voltage

This section is dedicated to the simultaneous analysis of constant power and constant voltage loads. In the first step, both loads are examined without any controllers. Subsequently, the analysis is conducted with the presence of PID and FOPID controllers, as well as noise. Figure 14 shows the overall schematic of the constant power and constant voltage loads simultaneously, without any controllers or noise. Figure 15 shows the output power under a constant voltage and power loads condition. This section investigates the simultaneous presence of constant power and constant voltage loads. In this scenario, both loads are initially examined without any control systems in place. Figures 16 and 17 illustrate the line voltage and output voltage waveforms under constant voltage and constant power load conditions.

As observed, without a voltage controller, the bus voltage sags and fails to track the 250-volt reference. Moreover, the voltages of both the constant power and constant voltage loads exhibit instability, with a significant overshoot in the constant power load voltage. Figure 18 presents the output power under both constant power and constant voltage load conditions, incorporating a PID controller.

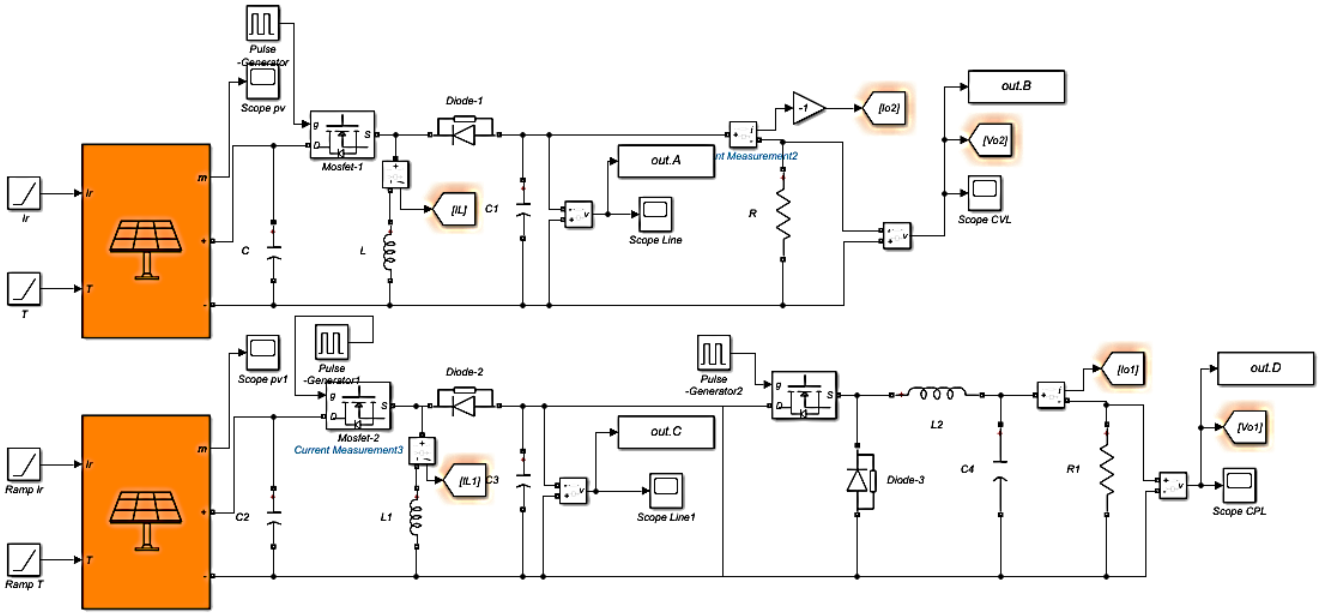

Fig. 14. Constant Power Load and Constant Voltage Load (CPL and CVL).

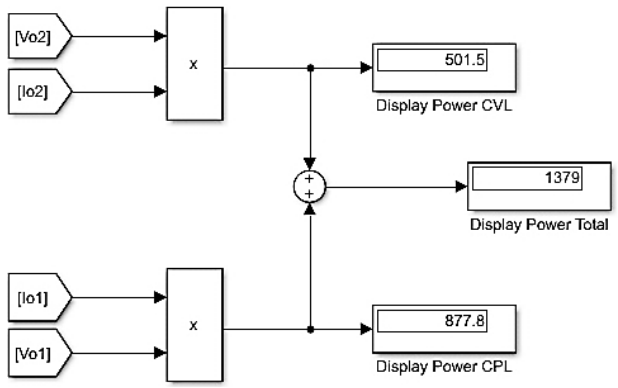

Fig. 15. Power CPL and CVL.

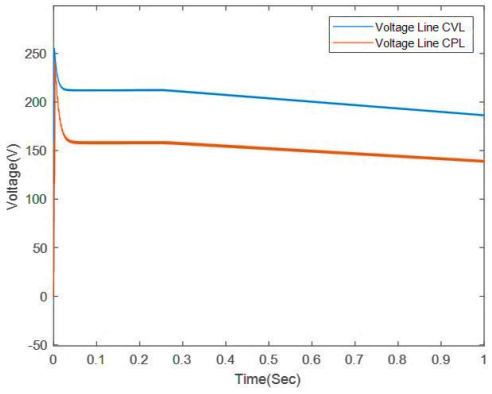

Fig. 16. Voltage line.

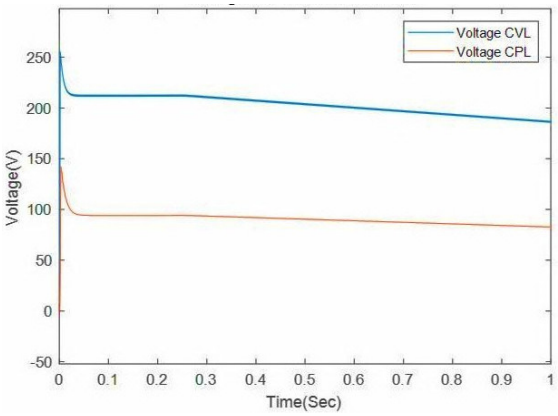

Fig. 17. Output CPL and CVL.

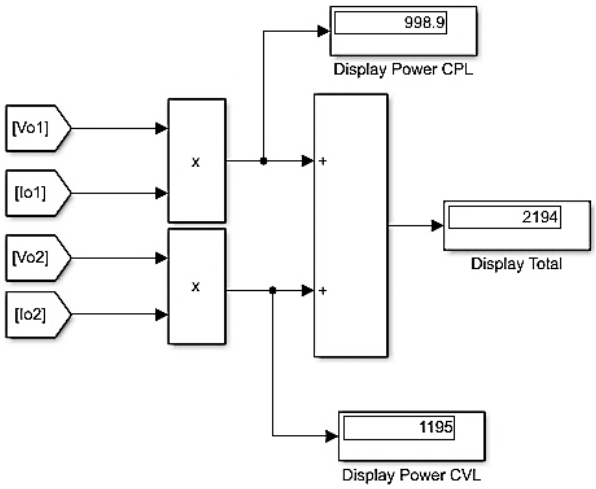

Fig. 18. Power CPL and CVL With a PID controller.

Figure 19 shows the output line voltage in both constant power and constant voltage load conditions with the presence of a PID controller. With the help of the controller, the buck-boost output has been able to approximate the desired output line voltage of 250 volts to some extent. Figure 19 shows the output line voltage in both constant power and constant voltage load conditions with the presence of a PID controller. Figure 20 presents the output voltages under constant power and constant voltage load conditions with a PID controller. Considering the constant voltage load condition, the output is proportional to the line output, and the output of the constant power load reaches the desired value according to the modeled condition. However, as it is clear from the results, the PID controller is much slower in the steady and transient states. On the other hand, the PID controller is not resistant to noise and system parameter changes.

Figure 21 presents the output power under both constant power and constant voltage load conditions, incorporating an FOPID controller. Figure 22 shows the line output voltages of the constant power and constant voltage loads in the presence of an FOPID controller.

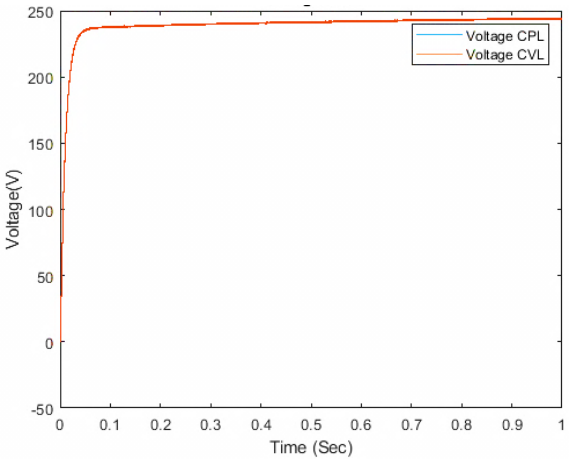

Fig. 19. Voltage line CPL and CVL With a PID controller.

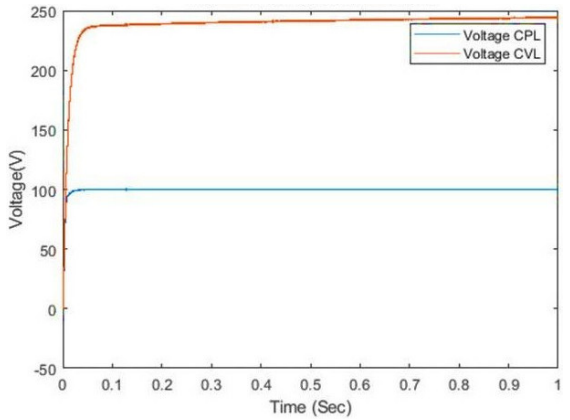

Fig. 20. Output CPL and CVL With a PID controller.

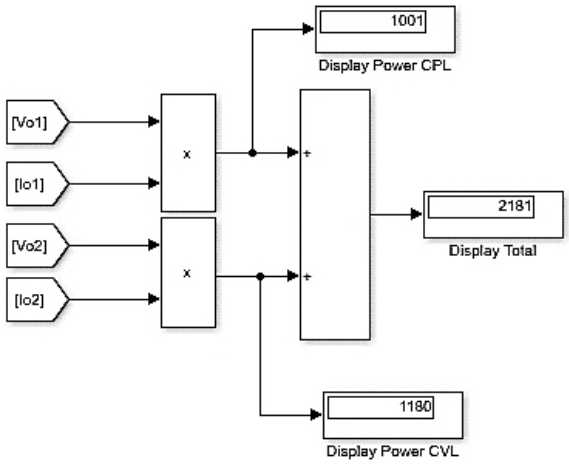

Fig. 21. Power CPL and CVL with a FOPID controller.

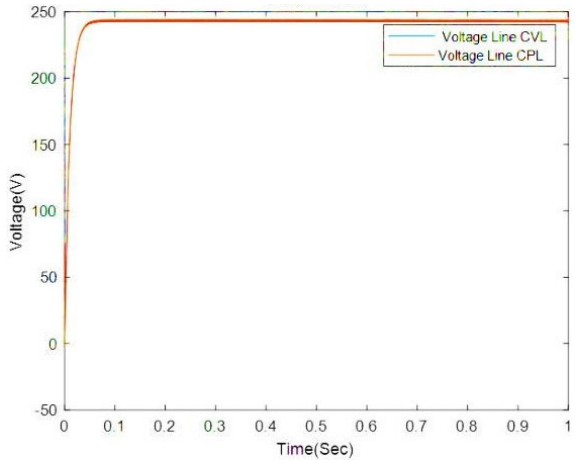

Fig. 22. Voltage line CVL and CPL with a FOPID controller.

The buck-boost output with the FOPID controller is able to reach the line output of 250V faster, indicating a better performance of the FPID controller in this section. Figure 23 shows the output voltages of the constant power and constant voltage loads in the presence of an FOPID controller, and based on the trend of this figure, the controller has been able to adjust the output of the loads proportionally to the line output.

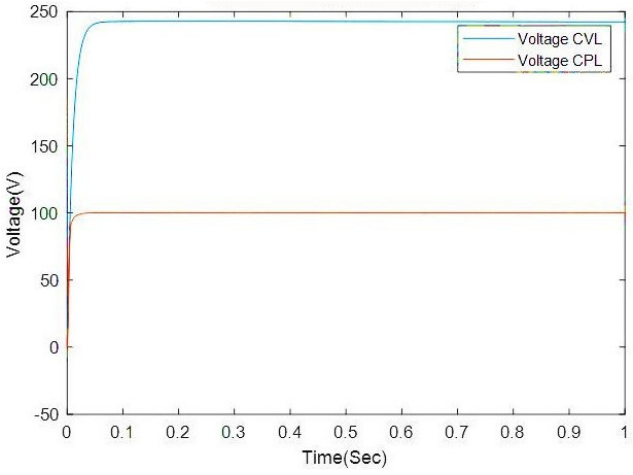

Fig. 23. Output CPL and CVL with a FOPID controller.

In the next step, the presence of noise in the presence of controllers is investigated, which can be used to evaluate the controller's performance in the presence of noise. It should be noted that the reason for choosing this condition is that noise is a major problem in electronic circuits that can affect circuit performance. Therefore, in this paper, the performance of PID and FOPID controllers against noise is analyzed with the aim of reducing the adverse effects of noise. Figure 24 presents the output power under both constant power and constant voltage load conditions, incorporating a PID controller, while also demonstrating the impact of noise.

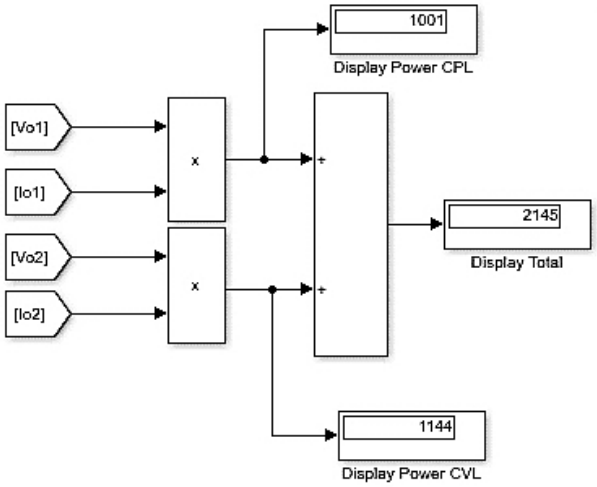

Fig. 24. Power CPL and CVL with PID controller with noise.

Figure 25 shows the line output voltage under constant power and constant voltage load conditions with a PID controller along with noise. As seen in the figure, the controller has been able to maintain a stable line output voltage despite the presence of noise.

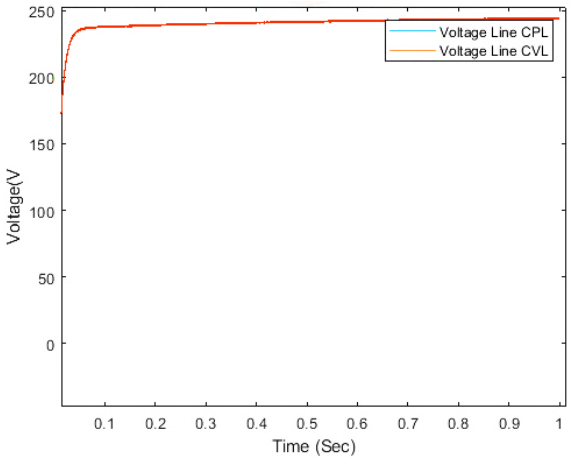

Fig. 25. Voltage line CPL and CVL with PID controller and noise.

Figure 26 shows the output voltage under constant power and constant voltage load conditions with a PID controller along with noise. The output voltage has also remained unchanged due to the good performance of the controller, even in the presence of noise. Figure 27 shows the output power with an FOPID controller for constant power and constant voltage loads, including noise. Figure 28 illustrates the output voltage of the lines under constant power load and constant voltage conditions with the presence of an FOPID controller

and noise. The output voltage of the line has exhibited better performance in the presence of noise as it is much closer to the desired value of 250 volts.

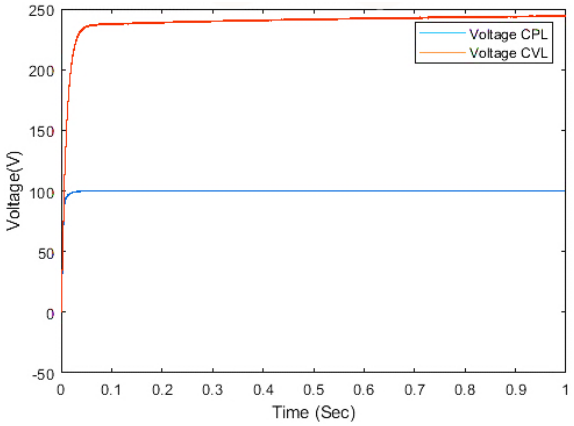

Fig. 26. Output CPL and CVL with PID controller and noise.

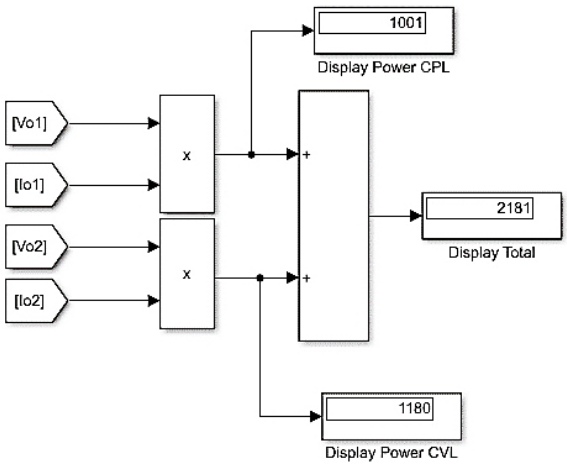

Fig. 27. Power CPL and CVL with FOPID controller and noise.

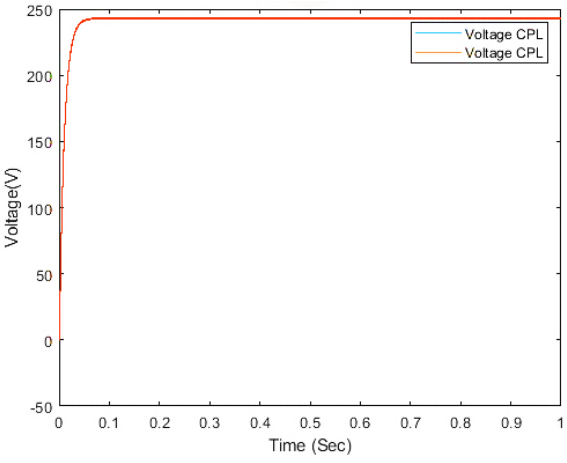

Fig. 28. Voltage Line CPL and CVL with FOPID controller.

Figure 29 clearly shows that the output voltage of both the constant power load and the constant voltage load is also closer to the desired value in the presence of noise. Studies conducted in the presence of noise and controllers indicate that the controllers are robust against noise and can provide satisfactory output in the face of noise in the simulated circuit. In the next step, the constant power load and the constant voltage load were simultaneously considered. Figures 30 and 31 show the output of the lines with two controllers under constant power and constant voltage loads. Based on these two figures, the FOPID controller has a more stable and faster response compared to the PID controller and reaches 250 volts. Figures 32 and 33 show the output voltage of the constant power load and the constant voltage load, where both controllers have the same output under constant power load, but under constant voltage load, the FOPID controller has shown a more stable and faster performance.

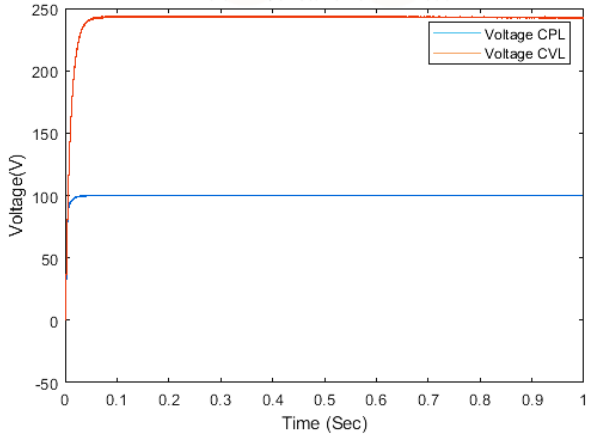

Fig. 29. Output CPL and CVL with FOPID controller.

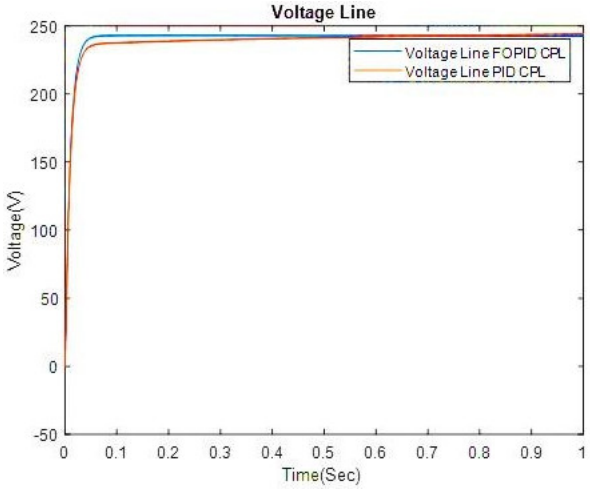

Fig. 30. Voltage line CPL with PID and FOPID controller.

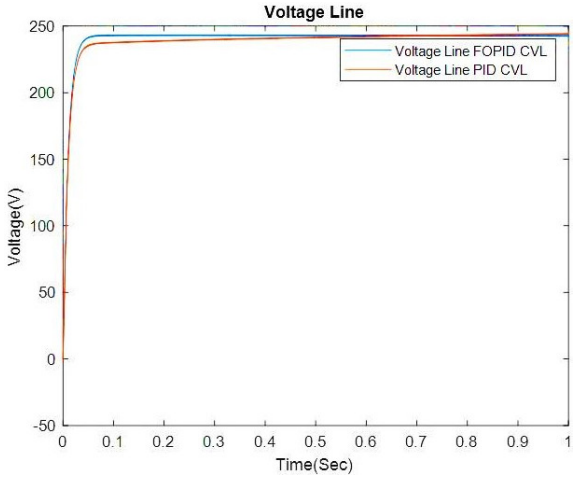

Fig. 31. Voltage line CVL with PID and FOPID controller.

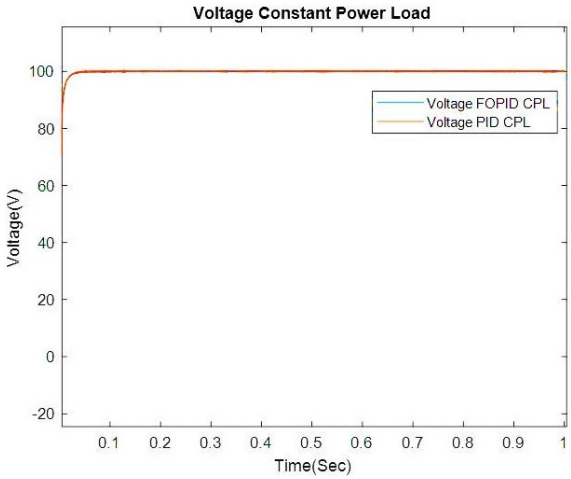

Fig. 32. Output CPL with PID and FOPID controller.

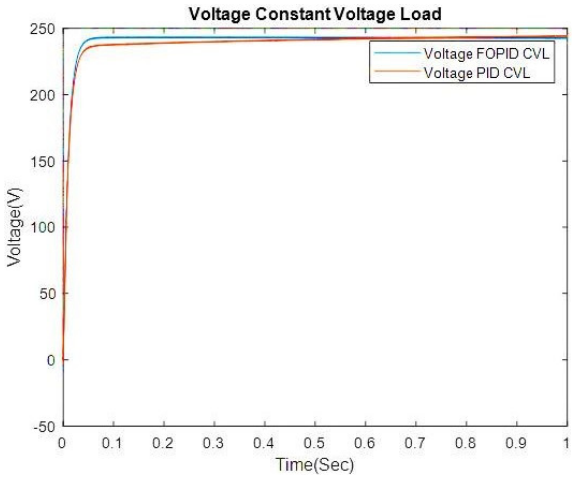

Fig. 33. Output CVL with PID and FOPID controller.

In the final section, the performance of controllers is analyzed for the presence of both constant power and constant voltage loads simultaneously, under noisy conditions. Figures 34 and 35 show the load line outputs in the presence of two controllers and noise. The FOPID controller exhibits more stable and faster performance compared to the PID controller. Figures 36 and 37 show the load outputs, where both controllers have the same output for the constant power load. However, in the case of the constant voltage load, it can be observed that the FOPID controller performs faster despite noise. The amount of rise time of PID and FOPID controller is written in Table 1. The Fractional Order Proportional-Integral-Derivative controller demonstrates superior performance in specific scenarios due to its inherent flexibility and robustness. Unlike traditional PID controllers, which use integer-order derivatives and integrals, FOPID controllers employ fractional calculus, allowing for more nuanced control dynamics. The fractional orders of the integrative and derivative components provide additional degrees of freedom, enabling more precise tuning. This is particularly beneficial in systems with complex dynamics, such as DC microgrids with variable loads and renewable energy sources. Fractional order controllers can better handle system uncertainties and external disturbances. This is crucial in microgrids, where power generation and consumption can be highly unpredictable due to fluctuating solar irradiance and temperature. Additionally, fractional calculus incorporates a memory effect, meaning the controller's response depends on the entire history of the system's behavior, not just the current state. This characteristic allows for more accurate and stable control in systems with time-varying properties. Furthermore, FOPID controllers offer superior performance in the frequency domain, providing better phase and gain margins and resulting in improved stability and transient response. By leveraging these theoretical advantages, the FOPID controller can achieve more stable and efficient control in DC microgrids, making it a more effective solution than conventional PID controllers.

6 Conclusions

This paper presents a comprehensive review of previous works on the control and stabilization of DC microgrids. Subsequently, the proposed model, research objectives, the studied system, and its limitations are explained. Then, the proposed controller algorithms and design are presented. Simulations of various scenarios have been successfully conducted using MATLAB software on a sample DC microgrid.

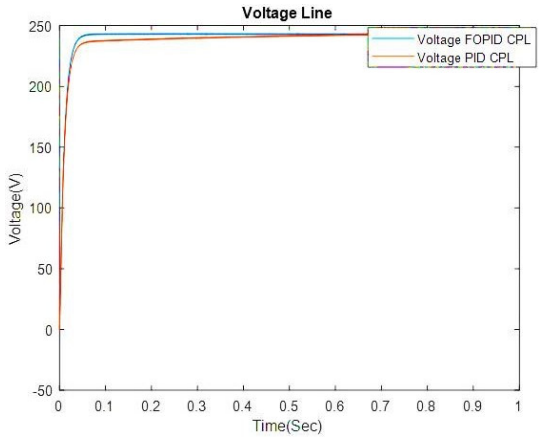

Fig. 34. Voltage Line CPL with PID and FOPID controller with noise.

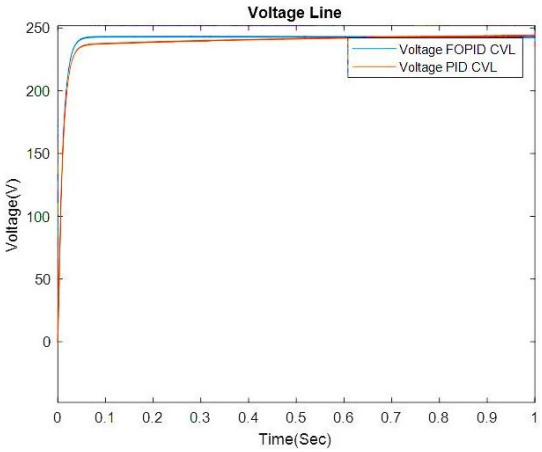

Fig. 35. Voltage Line CPL with PID and FOPID controller with noise.

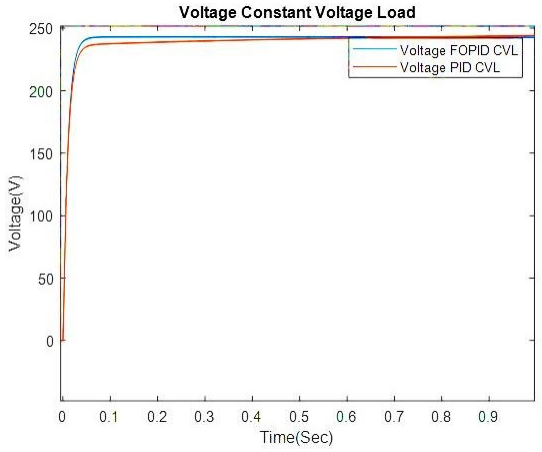

Fig. 36. Output CVL with PID and FOPID controller with noise.

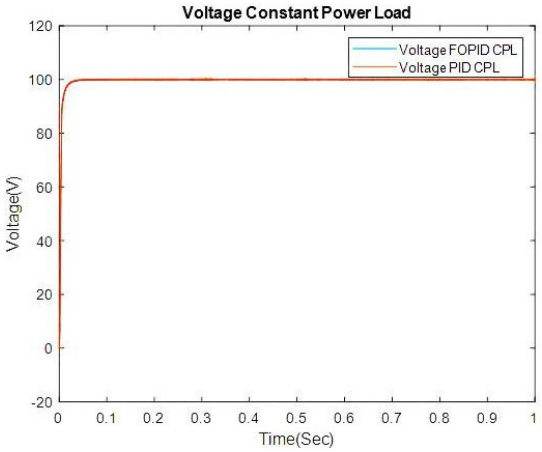

Fig. 37. Output CVL with PID and FOPID controller with noise.

Table 1. Comparison between PID and FOPID controllers in rise time.

Controllers	Rise Time
The proposed FOPID	0.1 second
PID	0.4 second

The results demonstrate that the FOPID controller exhibits better stability and faster response compared to the PID controller. Due to its higher degree of freedom, the FOPID controller shows better robustness against noise and parameter variations compared to the PID controller. Based on the simulation results, the FOPID controller is a suitable option for controlling and stabilizing DC microgrids. Additionally, the presence of two controllers has led to a final load consumption of 2 kW, whereas the load consumption of constant power and constant voltage loads is lower without the controllers. While the optimization of the fractional order controller using the gray wolf optimization algorithm shows promise, there are several limitations to consider. Firstly, the GWO algorithm, like other metaheuristic methods, may require significant computational resources, especially for large-scale or highly complex systems. This can limit its practical application in real-time scenarios. Secondly, the performance of GWO can be sensitive to the choice of parameters, and finding the optimal settings may require extensive trial and error. Additionally, while GWO is effective in avoiding local optima, it may still struggle with convergence speed, potentially leading to

longer optimization times. Another limitation is the assumption of ideal conditions in simulations, which may not fully capture the variability and unpredictability of real-world environments. Finally, the research may not account for all possible disturbances and uncertainties in a DC microgrid, which could affect the robustness and reliability of the optimized controller in practical applications. Addressing these limitations in future work could enhance the applicability and effectiveness of the GWO-optimized fractional order controller. The results demonstrate that:

- The FOPID controller outperforms the PID controller.
- The FOPID controller exhibits faster response and closer tracking to the 250V reference in both constant power load and constant voltage load conditions.
- The FOPID controller demonstrates better stability in the presence of noise and effectively protects the output from noise disturbances.
- The FOPID controller is a better choice for controlling buck-boost converters in DC microgrids, especially those based on solar panels.
- The presence of two controllers has enabled the load consumption to reach a final value of 2 kW, whereas without the controllers, the load consumption in constant power and constant voltage load conditions was lower.

The implementation of fractional order controllers in microgrids has shown significant improvements in stability and efficiency. Future research should focus on optimizing these controllers for diverse operating conditions and integrating advanced renewable energy sources. Field work will be crucial in validating theoretical models and ensuring practical applicability. Continued efforts in this area promise to enhance the reliability and sustainability of microgrid systems.

References

[1] Xiao J, Wang P, Setyawan L. Hierarchical control of hybrid energy storage system in DC microgrids. IEEE Transactions on Industrial Electronics. 2015;62(8):4915–4924.

[2] Byeon G, Yoon T, Oh S, Jang G. Energy management strategy of the DC distribution system in buildings using the EV service model. IEEE Transactions on Power Electronics. 2012;28(4):1544–1554.

[3] Su M, Liu Z, Sun Y, Han H, Hou X. Stability analysis and stabilization methods of DC microgrid with multiple parallel-connected DC–DC converters loaded by CPLs. IEEE Transactions on Smart Grid. 2016;9(1):132–142.

[4] Patil MD, Vadirajacharya K, Khubalkar SW. Design and tuning of digital fractional-order PID controller for permanent magnet DC motor. IETE Journal of Research. 2023;69(7):4349–4359.

[5] Warrier P, Shah P. Fractional order control of power electronic converters in industrial drives and renewable energy systems: a review. IEEE Access. 2021;9:58982–59009.

[6] Naidu RPK, Meikandasivam S. Power quality enhancement in a grid-connected hybrid system with coordinated PQ theory & fractional order PID controller in DPFC. Sustainable Energy, Grids and Networks. 2020;21:100317.

[7] Xue D, Chen Y. A comparative introduction of four fractional order controllers. In: Proceedings of the 4th World Congress on Intelligent Control and Automation (Cat. No. 02EX527). vol. 4. IEEE; 2002. p. 3228–3235.

[8] Khorsandi A, Ashourloo M, Mokhtari H. An adaptive droop control method for low voltage DC microgrids. In: The 5th Annual International Power Electronics, Drive Systems and Technologies Conference (PEDSTC 2014). IEEE; 2014. p. 84–89.

[9] Radwan AAA, Mohamed YARI. Linear active stabilization of converter-dominated DC microgrids. IEEE Transactions on Smart Grid. 2011;3(1):203–216.

[10] Gholizade-Narm H. A novel control strategy for a single-phase grid-connected power injection system. International Journal of Engineering-Transactions C: Aspects. 2014;27(12):1841–1849.

[11] Jin C, Wang P, Xiao J, Tang Y, Choo FH. Implementation of hierarchical control in DC microgrids. IEEE transactions on industrial electronics. 2013;61(8):4032–4042.

[12] Hassan MA, He Y. Constant power load stabilization in DC microgrid systems using passivity-based control with nonlinear disturbance observer. IEEE access. 2020;8:92393–92406.

[13] Soriano-Rangel CA, He W, Mancilla-David F, Ortega R. Voltage regulation in buck–boost converters feeding an unknown constant power load: An adaptive passivity-based control. IEEE Transactions on Control Systems Technology. 2020;29(1):395–402.

[14] Jeung YC, Lee DC, Dragičević T, Blaabjerg F. Design of passivity-based damping controller for suppressing power oscillations in DC microgrids. IEEE Transactions on Power Electronics. 2020;36(4):4016–4028.

[15] Mishra D, Nayak PC, Prusty RC. PSO optimized PIDF controller for Load-frequency control of AC Multi-Islanded-Micro grid system. In: 2020 International Conference on Renewable Energy Integration into Smart Grids: A Multidisciplinary Approach to Technology Modelling and Simulation (ICREISG). IEEE; 2020. p. 116–121.

[16] Seo SW, Choi HH. Digital implementation of fractional order PID-type controller for boost DC–DC converter. IEEE Access. 2019;7:142652–142662.

[17] Chen X, Pei W, Tang X. Transient stability analyses of micro-grids with multiple distributed generations. In: 2010 International Conference on Power System Technology. IEEE; 2010. p. 1–8.

[18] Nasraoui K, Lakhoua N, El Amraoui L. Study and analysis of micro smart grid using the modeling language SysML. In: 2017 International Conference on Green Energy Conversion Systems (GECS). IEEE; 2017. p. 1–8.

[19] Dragičević T, Guerrero JM, Vasquez JC, Škrlec D. Supervisory Control of an Adaptive-Droop Regulated DC Microgrid With Battery Management Capability. IEEE Transactions on Power Electronics. 2014;29(2):695–706.

[20] Obara S. Optimum Design of Renewable Energy Systems: Microgrid and Nature Grid Methods. Engineering Science Reference; 2014.

[21] Mhankale SE, Thorat A. Droop control strategies of DC microgrid: A review. In: 2018 International Conference on Current Trends towards Converging Technologies (ICCTCT). IEEE; 2018. p. 372–376.

[22] Wang F, Duarte JL, Hendrix MA, Ribeiro PF. Modeling and analysis of grid harmonic distortion impact of aggregated DG inverters. IEEE transactions on power electronics. 2010;26(3):786–797.

[23] Hambley AR. Electrical engineering: principles and applications. vol. 4. Prentice Hall; 2017.

[24] Tseng SY, Chen CC, Wang HY. Buck-Boost/Forward Hybrid Converter for PV Energy Conversion Applications. International Journal of Photoenergy. 2014;2014(1):392394.

[25] Bhan V, Hashmani AA, Memon AH. An Optimized Proportional Integral Derivative (PID) based Power System Stabilizer (PSS) for Damping of Active Power Oscillations. Sukkur IBA Journal of Emerging Technologies. 2022;5(2):42–48.

[26] Somefun OA, Akingbade K, Dahunsi F. The dilemma of PID tuning. Annual Reviews in Control. 2021;52:65–74.

[27] Zhao C, Xue D, Chen Y. A fractional order PID tuning algorithm for a class of fractional order plants. In: IEEE international conference mechatronics and automation, 2005. vol. 1. IEEE; 2005. p. 216–221.

[28] Sarvi M, Avanaki IN. An optimized fuzzy logic controller by water cycle algorithm for power management of stand-alone hybrid green power generation. Energy conversion and management. 2015;106:118–126.

[29] Khodabakhshian A, Esmaili MR, Bornapour M. Optimal coordinated design of UPFC and PSS for improving power system performance by using multi-objective water cycle algorithm. International Journal of Electrical Power & Energy Systems. 2016;83:124–133.

[30] Shadravan S, Naji HR, Bardsiri VK. The Sailfish Optimizer: A novel nature-inspired metaheuristic algorithm for solving constrained engineering optimization problems. Engineering Applications of Artificial Intelligence. 2019;80:20–34.

[31] Qu L, Hu H, Huang Y. Fractional order PID controller based on particle swarm optimization implemented with FPGA. In: 2010 International Conference on Artificial Intelligence and Computational Intelligence. vol. 1. IEEE; 2010. p. 165–169.

[32] Gupta S, Deep K. A novel random walk grey wolf optimizer. Swarm and evolutionary computation. 2019;44:101–112.

[33] Faris H, Aljarah I, Al-Betar MA, Mirjalili S. Grey wolf optimizer: a review of recent variants and applications. Neural computing and applications. 2018;30:413–435.